International
Journal
Of Advanced Research in Engineering& Management (IJAREM)
ISSN: 2456-2033 || PP. 06-14

Effects of Static Magnetic Field on Power Output in Silicon Polycrystalline Solar Cell

Ndeto M.P[1]*, Kinyua R[2], Ngaruiya J.M[3]
[1] *Institute of Energy and Environmental Technology, Jomo Kenyatta university of Agriculture and Technology P.O. Box 62000-00200, Nairobi.*Corresponding author*
[2] *Institute of Energy and Environmental Technology, Jomo Kenyatta university of Agriculture and Technology P.O. Box 62000-00200, Nairobi.*
[3]*Department of Physics, Jomo Kenyatta university of Agriculture and Technology P.O. Box 62000-00200, Nairobi*

Abstract: Abundance of solar energy presents solar PV as the best energy solution for most developing countries to meet the energy needs of their growing population. Solar PV technology is rarely used as the major power source in most countries; this is due to their poor conversion efficiencies which are less than 30% and high production cost. This study reports variance of PV parameters for polycrystalline (pc-Si) module when subjected to a static magnetic field equivalent in magnitude to the earth's magnetic field. The magnitude of the magnetic field was varied from 0.00mT to 0.08mT. The Solar cell output current and voltage were obtained under indoor conditions then normalized to outdoor environmental conditions for both Standard Testing Conditions (STC) and Typical Module Operating Temperatures (TMOT). Experimental results showed that maximum power (P_{MPP}) obtainable from the module decreased considerably as a result of an increase in static magnetic field **B**, hence a decrease in the conversion efficiency (η).This decrease in η corresponds to an increase of $0.26m^2$on the aperture area per every Kilo-watt of electric power generated from pc-Si module in countries existing along the latitude 50^0N/S as compared to those found at the Equator 0^0.

Keywords: Conversion efficiency, Hall's voltage, Polycrystalline_solar cell, Standard Testing Conditions (STC), Static magnetic field, Typical Module Operating Temperature (TMOT).

1. Introduction

Powering today's industries and life styles under a clean environment creates a need for a green source of energy. Solar PV is such energy under renewable sources. Depletion of ozone layer is a consequence of the use of "unclean" sources of energy i.e. fossil fuels which lead to adverse climatic changes and global warming. The use of clean energy i.e. renewable energies creates a remedy for a clean environment.

Solar photovoltaic conversion tap an abundant resource that is free of charge and available everywhere in the world .The amount of energy supplied by the sun in one day is enough to cater for world's electric power demand in one year(Pandey & Singh, 2016). Despite the fact that photovoltaic (PV) is the most promising future energy technology among a wide variety of renewable energy projects, it has a large barrier impending to large scale power- source application. These barriers include low energy conversion efficiencies and high price of the solar module (Karakaya & Sriwannawit, 2015).

A design of a more efficient solar module through structural improvements may lead to a reduced aperture area therefore reducing the production cost.

1.1 Theoretical principles

The solar cell is a specially designed p-n junction or Schottky barrier device. When the solar cell is exposed to light a DC current is generated which varies linearly with the solar irradiance. Documented factors constituting the failures of a solar cell include; Cell temperature, maximum power point tracking (MPPT) and energy conversion efficiencies. An increase in temperature leads to a decrease in open circuit Voltage (V_{oc}) which lowers the output power. The energy conversion efficiency is increased by reduction on the reflection of incident light by; use of antireflective coating and optical confinement of incident light with textured surface.

Finally, the MPPT greatly affects the efficiency of the solar cell as it determines its spectral response. The optimization of PV modules help in aligning the PV cell array in order to operate at the maximum power point(Meral & Din, 2010).

Series and shunt resistances are important parameters in the performance of a solar cell. According to Barro (2015), shunt resistance increases with an increase in magnetic field. This increase becomes less significant when the magnetic field **B** becomes high. On the other hand the series resistance at low magnetic field; less than 10^{-5}T, is low and almost constant. A further increase in magnetic field will lead to an increase in the series resistance. This is due to the fact that the blocking of the minority charge carriers becomes significant due to the presence of magnetic field thus a reduced photocurrent(Barro, 2015).

The simulated magnetic field under this study is equivalent in magnitude to the Earth's magnetic field. The total magnetic field (total intensity) on the earth surface has a minimum value of **0.022 milli-Tesla (mT**) and a maximum value of **0.067milli-Tesla (mT)** valid from 2015.0 to 2020.0. The strength of the geomagnetic field at the 0^0 latitude (at the equator) and the 50^0 latitude is approximately **0.031mT** and **0.058mT** respectively(Maus, Nga, Macmillan, & Thomson, 2015).

When a magnetic field transverses through a current *I* flowing through a conducting strip of rectangular section at right angles to the direction of the current, a voltage called Hall Voltage is produced between two superposed points on the opposite side of the strip. A theoretical calculation of the Hall voltage in a solar cell subjected to a static magnetic field equivalent to the earth's magnetic field is 2.482mV at a magnetic field of 0.031mT and 4.644mV at a magnetic field of 0.058mT, from Eqn.6(Meral & Din, 2010).

Semiconductors depend on electrons and holes for conductivity. Conductivity in materials entirely depends on carrier density. Materials with a lower carrier density exhibits Hall Effect more strongly for given current and depth, *t*. Silicon, germanium and gallium – arsenide provide the low carrier densities needed to realize this effect.

1.2 Mathematical models for normalizing output parameters

In order to simulate a near outdoor conditions factoring in the cell temperature in a laboratory setting, the output parameters were normalized to STC and TMOT. This is in accordance with the International Electrotechnical Commission's (IEC) international standards for crystalline Si terrestrial photovoltaic module testing (IEC TS 62257). Eqn.1a and 1b below were used to normalize the output current.

$$I = I_m \times \frac{1000W/m^2}{G} \quad \text{(STC)} \qquad (1a)$$

$$I = I_m \times \frac{1061W/m^2}{G} \quad \text{(TMOT)} \qquad (1b)$$

Where *I* is the PV module's current and I_m is the measured current in amperes (A) and *G* is the measured incident solar irradiance during the I-V curve measurement, in watts per square metre (W/m^2).

The temperature coefficient for the voltage ($T_{C,VOC}$) was determined by the formula

$$T_{C,VOC} = \frac{(V_{OC,1} - V_{OC,2})/V_{OC,2}}{T_1 - T_2} \qquad (2)$$

Where $T_{C,VOC}$ is the PV module's temperature coefficient for the voltage, per degree Celsius ($1/^0C$) ,$V_{OC,1}$ is the PV module's open circuit voltage immediately after exposure to sunlight, $V_{OC,2}$ is the PV module's open circuit voltage after the I-V measurement is taken, T_1 is the PV module's temperature immediately before exposure to sunlight and T_2 is the PV module's temperature after the I-V measurement is taken.

All the voltage measurements were converted to STC by using the following formula

$$V = V_m[1 + T_{C,VOC}(T_{STC} - T)] \qquad (3)$$

Where *V* is the PV module's Voltage at STC and V_m is the measured voltage, $T_{C,VOC}$ is the PV module's temperature coefficient for the voltage, per degree Celsius ($1/^0C$), T_{STC} is the temperature at STC(25^0C), T_{TMOT} is the temperature at TMOT (50^0C) and *T* is the PV module's temperature during the I-V curve measurements.

The PV module's measured maximum power point power at STC (P_{MPP}) was calculated using the formula

$$P_{MPP} = I_{MPP}V_{MPP} \qquad (4)$$

The solar cell power conversion efficiency, □ was calculated by the ratio of maximum power point, $\mathbf{P_{mpp}}$ to the input irradiance (**E**, in W/m^2) under STC and the surface area of the solar cell, ($\mathbf{A_c}$ in m^2)(IEC,2016).

$$\eta = \frac{P_{MPP}}{(E \times Ac)} \qquad (5)$$

The values of Hall's Voltage were calculated using Eqn.6 below

$$|V_H| = \frac{I_x B_z}{nqt} \quad (6)$$

Where, $n = 5 \times 10^{21} m^{-3}$, $I_x = \text{current}$, $q = 1.602 \times 10^{-19} C$, $t = 80 \times 10^{-6} m$ (optimal thickness)
$B_z = \text{magnetic field}$

From (2), the temperature coefficient ($T_{C,VOC}$) = -0.00217/^{0}C ,where $V_{OC,1}$ = 6.96V, $V_{OC,2}$ = 6.69V , T_1= 32.5^{0}C and T_2 = 51.1^{0}C

2. Methodology

Two 40W incandescent light bulbs were used for irradiation with a constant irradiation of 626W/m^2. Solar power meter (TM-206) was used to measure the irradiance and infra-red thermometer (AD 5615) was used to monitor cell temperature during irradiation. The ambient temperature was 27.10 ± 0.80 and DPLIGHT 7V 3W (DP-P001&P002) polycrystalline_solar module (from China) was the sample module. TRI-KA (model no: X0220113242737) and TRI-SEN (model no: X0220113242737) were used to test and plot the I-V curves for the PV module with the Standard Test Condition (STC) being 1000W/m^2, 25^{0}C and A.M of 1.5 and Typical Module Operating Temperature (TMOT) being 1061W/m^2 and a temperature of 50^{0}C (IEC, 2016). The module area was 0.02m^2. Soft Iron ring was used to shield the solar cell from undesired ambient magnetic field.

3. Results, analysis and Discussion

3.1.1 Effects of Halls voltage $V_{H\_}$ as a result of variation of B on output voltage, V_m

A graphical analysis of the effects of Halls voltage on output Voltage is presented.

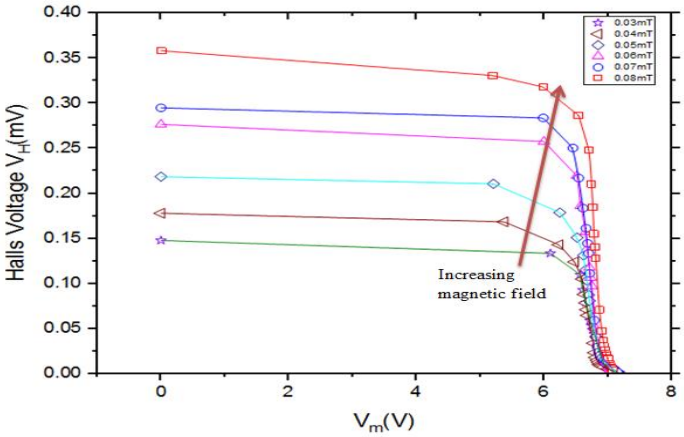

Fig.1: Graphical analysis of $V_{H\_}$ as a function of V for different **B**

Analysis of Fig.1 shows a variance in the values of V_H intercept and a near constant V_m intercept (V_{OC}). The 'knee' of the curves shifts upwards as a result of an increase in **B**. The shapes of the different curves in Fig.1show that $V_{H\_}$ is maximal for higher values of **B** and has a marginal effect on the values of V_m as they approach V_{OC}. However, a further analysis on V_H against I_m is required for a clearer deduction on the effects of V_H on the solar cell parameters.

3.1.2 Effects of Halls voltage V_H on output current, I_m as a result of variation of B

The Hall's Voltage is plotted against the output current in Fig.2 below for different values of magnetic field intensity.

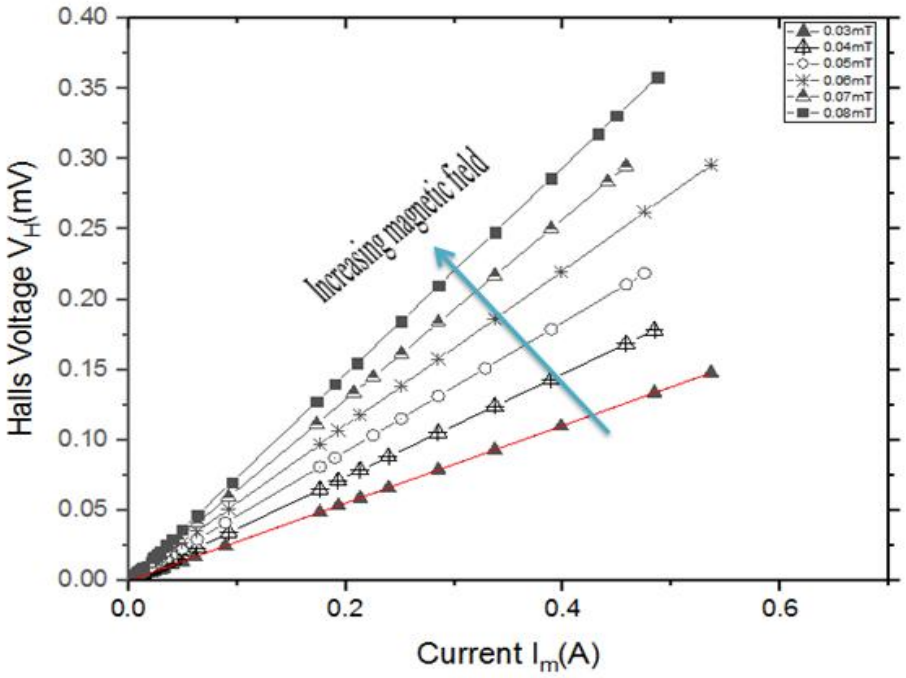

Fig.2: Graphical analysis of V_H (mV) against I_m (A) at STC in **B**

The graphs in Fig.2 show a linear relationship between V_H and I_m for different values of **B**. This corresponds to an increase in the slope of the graphs as the magnetic field increases. The slope increases with an average factor of 0.00026 for every 0.01mT increase in magnetic field. From Eqn.6, the magnitude of V_H is directly proportional to I_m at a constant magnetic field. From the graphs in Fig.2 the relationship shown in equations 7 and 8 below can be deduced.

$$V_H = \propto I_m \tag{7}$$

Where α = proportionality factor which is an increasing function of the magnetic field **B**.
Therefore α is proportional to **B** and can be expressed in the form;

$$\propto = \eta \boldsymbol{B} \tag{8}$$

Where η = constant and **B** is the magnetic field.
From Eqn.7 and 8, α can be expressed as

$$\propto = \frac{\Delta V_H}{\Delta I_m} = \eta \boldsymbol{B} \tag{9}$$

Therefore,

$$V_H = \eta \boldsymbol{B} I_m \tag{10}$$

A further analysis of the graph of $\propto$ as a function of **B** (Eqn.8) is presented in Fig.3 below.

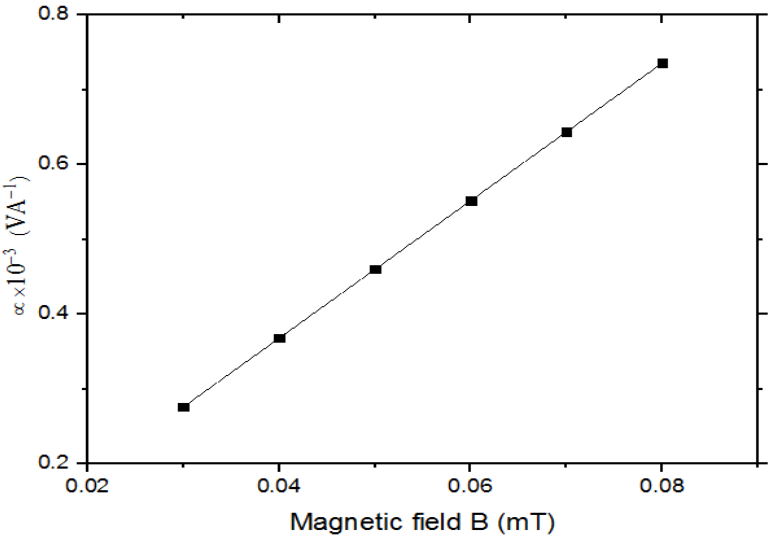

Fig.3: Graphical analysis of ∝ as a function of **B**

Fig.3 shows a graph of ∝ as a function of **B**. From an analysis of Eqn.8 and the slope of Fig.3, it can be concluded that the slope in Fig.3 represents η in Eqn.8.Therefore, the numerical value of η = (9.19977 ± 0.00448) $VA^{-1}T^{-1}$. According to Zerbo (2016), the quantity of charge carriers crossing the cell junction are greatly hindered by presence of magnetic field. An increase in **B** leads to an increase in deviation of charge carriers which lead to the generation of V_H; this explains the relation stated in Eqn.8. The generation of V_H creates a resistance like effect to the flow of charges across the junction which inhibits carrier mobility. This resistive behavior is referred to as magnetoresistance MR (Combari, Zerbo, Zoungrana, Ramde, & Bathiebo, 2017). There are many effects contributing to magnetoresistance MR. These effects encompasses physical and geometric contributions. Physical contributions are as a result of magnetic field dependence on carrier mobility, energy-band structure or spin-spin interactions, while geometric contribution arise from shape dependence and inhomogeneities of conductivities in the structure (Sun & Kosel, 2013). According to Sun (2013), the resistance in this case is a function of **B** and therefore explains the shifts in the values of the gradients in Fig.2.

Having observed some effects of **B** on magnetoresistance, there is a need to determine the extent of this effect on I_{mpp} and V_{mpp} which are the key parameters in determining the output power in a solar cell.

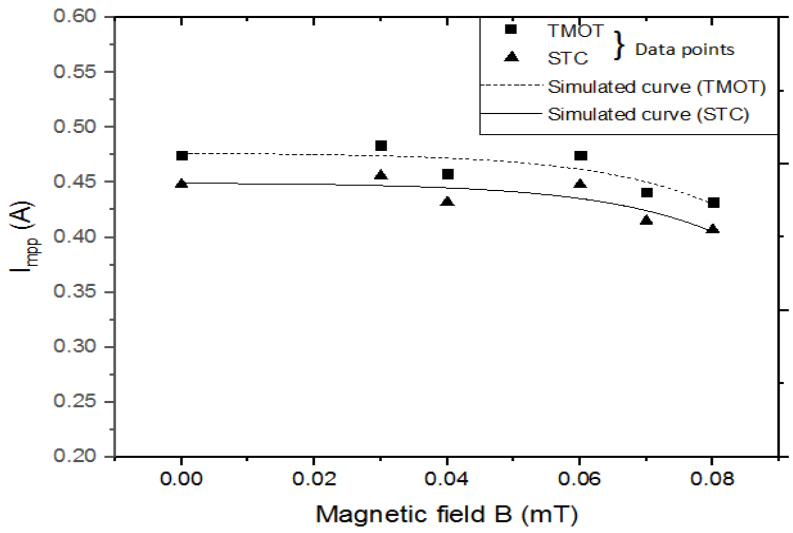

Fig.4: Graphical analysis of I_{mpp} [A] as a function of magnetic field **B** [mT]

Fig.4 shows a graph of I_{mpp} against **B** at STC and TMOT conditions. The graphs show a decrease in the optimal current (I_{mpp}) as a result of an increase in the magnetic field **B**. Light intensity has a dominant effect on current parameters. I_{SC} and I_{mpp} increase linearly as a consequence of an increasing light intensity (Nelson, 2003). An increase in irradiation from 1000W/m^2 at STC to 1061W/m^2 at TMOT explains the variance in the two curves as a function of **B**.

Zerbo (2015) observed that an increase in magnetic field leads to a reduction in the junction dynamic velocities which leads to a reduced solar cell operation point. This decrease is as a result of a reduced mean free path of the charge carriers as a consequence of an increase in magnetic field strength thus a change in the resistance of the solar cell. This explains the decrease in I_{mpp} as the magnetic field strength increases.

A further analysis of the effects of **B** on V_{mpp} is presented in Fig.5 below.

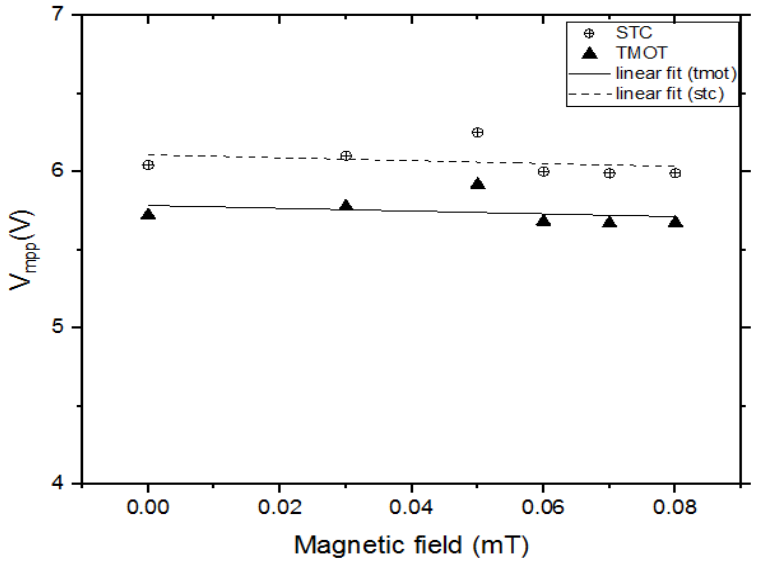

Fig.5: Graphical analysis of V_{mpp} [A] against magnetic field B [mT]

Fig.5 shows a graph of V_{mpp} as a function of **B**. A weak decrease in optimal voltage (V_{mpp}) is observed as **B** increases for both STC and TMOT conditions respectively. The values at STC appear higher than those at TMOT in Fig.5. Having normalized all data to STC (25^{0}C) and TMOT (50^{0}C), it is therefore expected that the values of V_{mpp} at STC should be higher than those at TMOT as depicted in Fig.5 due to a change in temperature(Cell, 2015).

From the above deductions it can be concluded that V_H has a noticeable decreasing effect on I_{mpp} and a weak effects on V_{mpp} for the values of **B** under this study. These findings are in agreement with studies conducted on bifacial solar module; although the magnitude of **B** differed, which stated that current at maximum power point decreased considerably and voltage increased weakly as a result of an increase in magnetic field (Combari et al., 2017).

3.1.3 Effects of Magnetic Field B on Power Output, Pm

Having analyzed I_{mpp} and $V_{mpp,}$ it is also important to quantify the effects of **B** on maximum power, P_{mpp}. An analysis of the shift in the maximum power and a comparison to the values of theoretical power P_T for both STC and TMOT conditions is presented in Fig.6 below.

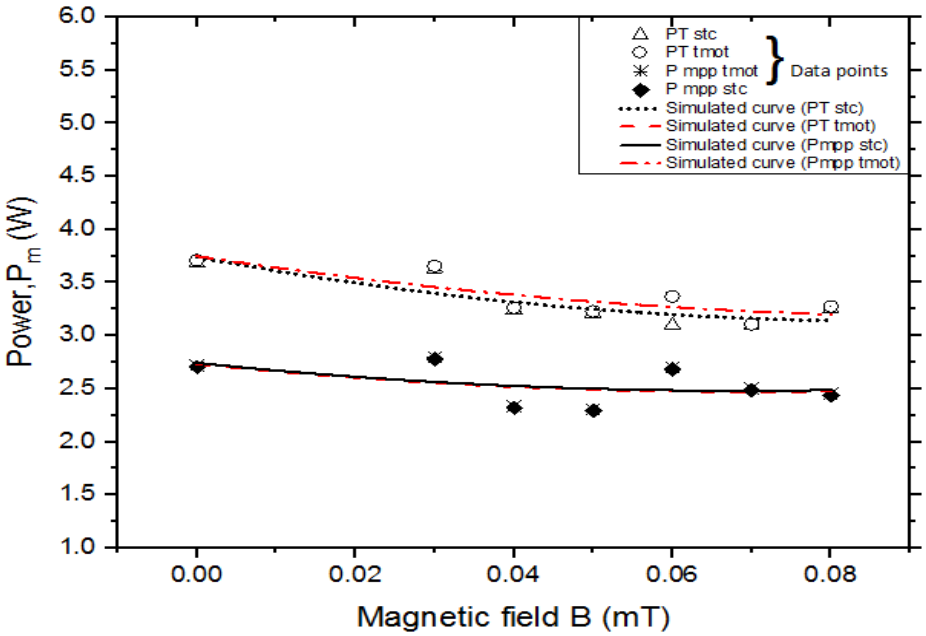

Fig.6: Graphical analysis of power (W) against magnetic field **B** (mT) for STC and TMOT

A considerable decrease in P_{mpp} and P_T as a result of increase in **B** is noted. It is observed that theoretical power P_T both at STC and TMOT lie above maximum power obtainable from the module. This decrease is attributed to magnetoresistance. Maximum electrical power generated also depends on junction dynamic velocities of charge carriers thus an increase in the load resistance(Zerbo, Zoungrana, Sourabié, Ouedraogo, & Zouma, 2016). A change in the junction dynamic velocities as a consequence of an increase in magnetic field greatly affects the solar cell operating point thus variance in the values of P_{mpp}. It is therefore evident that a slight variation in I_{mpp} and V_{mpp} would cause a shift on the values of P_{mpp} as illustrated in Eqn.4.

This decrease in P_{mpp} consequently may have some effects on the modules conversion efficiency η. This analysis is shown in Fig.7 below.

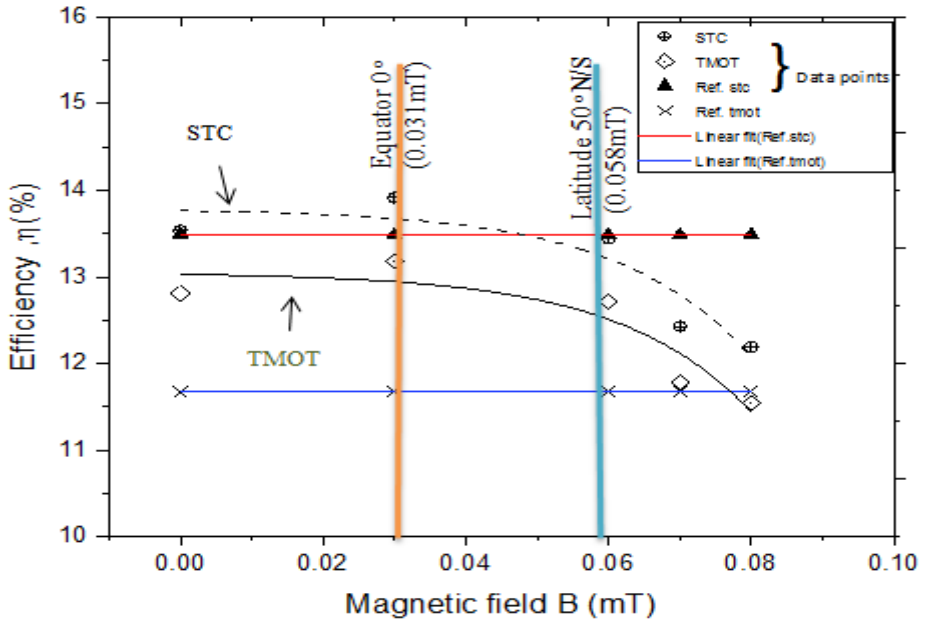

Fig.7: Graphical analysis of efficiency η (%) against magnetic field **B** (mT) for STC and TMOT

A comparison of pc-Si reference efficiencies and values of η in the presence of **B** at STC and TMOT respectively is presented. A noticeable decrease in η is observed for 0.03mT ≤ **B** ≤ 0.08mT. It is further observed that this decrease in conversion efficiency would be evidently felt in countries existing along latitudes experiencing the values of **B** shown above. This analysis is as a result of a superposition of the latitudes on the globe experiencing the same limit of earth's magnetic field as the one simulated in this study, on Fig.7.

It is now evident that an increase in magnetic field has a noticeable decreasing effect on the maximum electric power which consequently leads to a decrease in the pc-Si solar cell's conversion efficiency. This observation is in line with studies conducted on bifacial solar cell at a higher magnitude of magnetic field **B** (Combari et al., 2017).

3.1.4 Cost implication as a result of change in conversion efficiency as a consequence of magnetic field B

A change in conversion efficiency as a result of increase in magnetic field would have a cost implication on the production and purchase of a PV module. A graphical analysis of Fig.7 gives values of η at **B** = 0.031mT and 0.058mT which aid in quantifying the costs anticipated in comparison to documented cost of a pc-Si module tested under standard testing conditions of which magnetic field intensity is not inclusive.

Table 1 below shows a summary of the cost implications foreseen as a result of change in the conversion efficiency.

Table 1 Cost implication as a result of a change in conversion efficiency elicited by Δ**B**

	Rating	**Equator 0°**	**50° N/S Latitude**
Magnetic Field		0.031mT	0.058Mt
Current PV module lowest price/watt (USD/W)	$0.55		
Maximum PV module output power (W)	320.00	276.05	268.16
PV module size (m^2)	2.50	2.50	2.50
Area needed per kW (m^2)	7.81	9.06	9.32
Maximum PV efficiency (%)	15.00	12.94	12.57
decrease in efficiency		2.06	2.43
Cost per m^2 Module (USD)	$22.53		
Total Cost for a 1kW module(USD)	$176.00	$204.12	$209.98
Increase in cost (USD)		$28.12	$33.98

When a pc-Si module is operating at TMOT conditions in a country located along the equator, an aperture area of 9.06m^2 will be required for generation of 1Kw of electric power. This is due to the reduction of 2.06 on the conversion efficiency at 0.03mT as compared to the pc-Si modules' rating. Taking another town along the latitude of 50^0N/S of the equator experiencing the same conditions and **B** of 0.058mT, an aperture area of 9.32m^2 would be required. This change in the latitudes from 0^0 to 50^0 corresponds to a 0.26m^2 increment in the aperture area. This corresponds to a $5.86 increase in cost per Kilo-watt of electric power.

4. Conclusion

A theoretical study of the effects of static magnetic field on the electrical parameters of pc-Si solar module is presented .The voltage parameters and current parameters of the module have shown some considerable changes in the presence of static magnetic field. For instance, I_{mpp} decrease noticeably while V_{mpp} decrease weakly as a result of an increase in **B.** These changes are as a result of the effects of V_H on the carrier mobility which lead to an increase in the cell resistance in the presence of a magnetic field, an effect called magnetoresistance. These changes lead to a further decrease in the output power which consequently leads to a decrease in the pc-Si modules conversion efficiency.

From the above observations, it is evident that pc-Si solar modules perform better in areas having a lower value of the earth's magnetic field (equator 0^0), then decreases considerably towards higher latitudes. This

change in the conversion efficiency has a significant impact on the module's aperture area leading to a cost increment of 2.87% per Kilo watt of electric power in countries existing along 50^0N/S as compared to those at the Equator 0^0.

From the deductions made, it is of uttermost importance to include the value of magnetic field **B** as part of the Standard Testing Conditions in giving the ratings of pc-Si solar cell. In addition, studies can be conducted on the other types of solar modules (mono-crystalline, thin film and amorphous) so that a general conclusion can be made on the effects of static magnetic field on solar modules.

References

[1] Pandey, A., & Singh, D. K. (2016). Modelling of Photovoltaic Solar Panel for Maximum Power Point Tracking, *5*(5), 2015–2017.

[2] Karakaya, E., & Sriwannawit, P. (2015). Barriers to the adoption of photovoltaic systems : The state of the art, *49*, 60–66. http://doi.org/10.1016/j.rser.2015.04.058

[3] Meral, M., & Din, F. (2010). Critical Factors that Affecting Efficiency of Solar Cells. *Smart Grid and Renewable Energy*, *1*(1), 47. http://doi.org/10.4236/sgre.2010.11007

[4] Barro, F. I. (2015). Effect of both magnetic field and doping density on series and shunt resistances under frequency modulation, *53*(September), 590–595.

[5] Maus, S., Nga, C. R., Macmillan, S., & Thomson, A. (2015). The US / UK World Magnetic Model for 2010-2015. NOAA Technical Report NESDIS/NGDC. http://doi.org/10.7289/V5TB14V7

[6] IEC standard 62257-9: Photovoltaic Devices., Part 7: Computation of Spectral Mismarch Error Introduced in the Testing of a Photovoltaic Device, International Electrotechnical commission ,Geneva, 2016.

[7] Zerbo, I., Zoungrana, M., Sourabié, I., Ouedraogo, A., & Zouma, B. (2016). External Magnetic Field Effect on Bifacial Silicon Solar Cell ' s Electrical Parameters, (March), 146–151.

[8] Combari, D. U., Zerbo, I., Zoungrana, M., Ramde, E. W., & Bathiebo, D. J. (2017). Modelling Study of Magnetic Field Effect on the Performance of a Silicon Photovoltaic Module, 419–429. http://doi.org/10.4236/epe.2017.98028

[9] Sun, J., & Kosel, J. (2013). Extraordinary Magnetoresistance in Semiconductor/Metal Hybrids: A Review, 500–516. http://doi.org/10.3390/ma6020500

[10] Nelson, J. (2003). The Phisics of Solar Cells. *Properties of Semiconductor Materials*, 384. http://doi.org/10.1142/9781848161269_0001

[11] Cell, P. S. (2015). JnPs Effect of Temperature on the I-V Characteristics of a Polycrystalline Solar Cell. *Nepal Physical Society*, 35–40.

[12] Sector, V. P. (2012). Solar Photovoltaics. *International Renewable Energy Agency IRENA*,*1*(4).